

SYNTHETIC SEISMOGRAMS FOR SIMPLE "ALBERTA" MODELS¹

P.G. KELAMIS^{2, 3}, E.R. KANASEWICH² AND F. ABRAMOVICI⁴

ABSTRACT

The exact solution for a buried source is presented for a layer over a half space. An example which models the reflected and head waves from a Mississippian-type half space in a simplified "Alberta foothills" model is studied in detail. The computer algorithm evaluates a solution for a point vertical force based on the Cagniard - Pekeris formulation. The complete analytic solution is evaluated in terms of generalized rays, and it is shown that each ray may be examined individually or modified to incorporate the effects of attenuation. The attenuation effects are illustrated with a thin "weathered layer" model. In this model the near-field results are particularly interesting and have applications in shallow exploration problems. The exact solution for a point vertical or horizontal force shows the presence of a relatively unrecognized "surface head wave" beginning as a shear wave at the source and travelling as a P wave along the surface.

INTRODUCTION

Generalized ray theory was introduced formally into elastic wave problems by Pekeris *et al.* (1965). They describe the seismic wave solution as a double power series expansion over indices μ and ν ($\mu, \nu = 0, \dots, \infty$) in which each term in the expansion represents a ray that has been reflected μ times as a compressional (P) wave and ν times as a shear (S) wave. The expansion is carried out in the Laplace transform domain and has the following form

$$\bar{u}_i(p, r) = \frac{\bar{F}(p)}{4\pi\mu_1} \sum_{\mu=0}^{\infty} \sum_{\nu=0}^{\infty} \bar{G}_{\mu\nu}(p, r, i, j). \quad (1)$$

$i, j = 1, 2, 3$

The transformed displacements ($\bar{u}_1 = \bar{q}$, $\bar{u}_2 = \bar{v}$, $\bar{u}_3 = \bar{w}$) are in cylindrical coordinates (r, ϕ, z) in which circular symmetry is assumed for a model consisting of an elastic layer over a half space.

The velocities, densities and shear moduli in the two layers are $\alpha_1, \beta_1, \rho_1, \mu_1; \alpha_2, \beta_2, \rho_2, \mu_2$. The source response, \bar{F} , will be a vertical force produced by a jump in normal stress at a depth d below the surface in a layer of thickness H . The Laplace transform variable is $p (= i\omega)$ where ω is the angular frequency. The displacements in the time domain are obtained by an inverse Laplace transform following the method of Cagniard (1939) as generalized by Abramovici (1978).

The response of each generalized ray is given by \bar{G} , an integral involving integers μ and ν and the distance, r .

$$\bar{G}_{\mu\nu} = \int_0^{\infty} \frac{px^2}{\beta_1} \left[J_0 \left(\frac{prx}{\beta_1} \right) \left\{ R_i^P E_i + R_i^S F_i \right\} + J_0' \left(\frac{prx}{\beta_1} \right) \left\{ r_i^P e_i + r_i^S f_i \right\} \right] dx \quad (2)$$

where R_i^P and r_i^P are generalized reflection coefficients for the i th displacement for the totality of all rays starting as P and arriving at the receiver after being reflected μ times as P and ν times as S waves. Coefficients R_i^S and r_i^S play a similar role for rays starting as shear waves. E, e, F and f are spatial coefficients which are products of rational functions and exponential terms involving the velocities and the ratio of depth of source to layer thickness. The spatial coefficients determine the phase delay and the amplitude decay. For a vertical force, as used here, only the functions E_3, F_3, e_1 and f_1 are nonzero. The explicit relations for various sources are given in the theoretical papers by Abramovici (1970), Abramovici and Gal-Ezer (1978), and Abramovici, Kanasewich and Kelamis (1982).

¹ Paper presented at the CSEG National Convention, Calgary, Alberta, April 6, 1982.

² Department of Physics, University of Alberta, Edmonton, Alberta, Canada T6G 2J1.

³ Present address: Western Geophysical Company of America, P.O. Box 2469, Houston, Texas 77001.

⁴ School of Mathematical Sciences, Tel-Aviv University, Ramat-Aviv, Israel.

THE "ALBERTA" MODEL

Many sedimentary basins may be modelled, in a first approximation, as a thick, relatively uniform, low-velocity layer overlying a thick high-velocity section. A good example is the Alberta basin, which extends into the Rocky Mountains on the west. In the foothills it consists of a 3-km section of alternating shales and sands of Mesozoic age with a mean velocity of 4,200 m/s (13,800 ft/s) overlying Paleozoic and Precambrian beds with a mean velocity of 6,400 m/s (21,000 ft/s). The high velocity in the Paleozoic rocks is due to a large proportion of limestone and dolomite, whereas the Precambrian section, of similar velocity, consists of two-billion-year-old gneisses, metasediments and igneous intrusives.

The mean velocity contrast between the two sections is so large that special techniques may be used in mapping the contrast, as discussed by Blundun (1959) and Richards (1960). Nevertheless, identifying the phases used in mapping has been difficult because of the interference of many types of wide-angle reflections and head waves. Computing exact synthetic seismograms is also very difficult and has only recently been accomplished with large digital computers. Our own approach to this problem involves generalized ray theory and Cagniard-Pekeris inversion, because the method yields the complete and exact solution, and also allows the results to be decomposed into individual generalized rays for detailed analysis.

A concentrated vertical force at a particular depth is used instead of a buried compressional pulse, because a vibratory device or a cylindrically shaped tube of explosive chemical in a lightly tamped borehole produces a dominantly vertical force. Mathematically it is simulated by a jump in normal stress across a boundary at the source level placed on the z axis. The model of a buried source in a layer over a half space is a gross simplification of the actual crustal section in the Alberta basin. A more complex layered structure could be modelled, but with objectionable approximations in the algorithms or with prohibitively expensive computer operation. Before attempting these more elaborate models, the complexity of the results from these simpler examples will be explored.

The basic model used is given in Figure 1. Other velocities will be illustrated after the results for this case are shown. To obtain a perspective on the relative amplitudes, exact seismograms were computed for distances of 4 to 8 km from the source (Fig. 2). Rayleigh waves dominate the recording, and the earlier portion of the seismogram with the head and reflected waves is not seen clearly. As we are interested in this earlier section but at critical distances, we will restrict the display to the time before the surface waves arrive. Figure 3 shows the vertical and radial displacement for a vertical point force at distances of 8 to 20 km (5 to 12.4 mi). These may be compared to the field record-

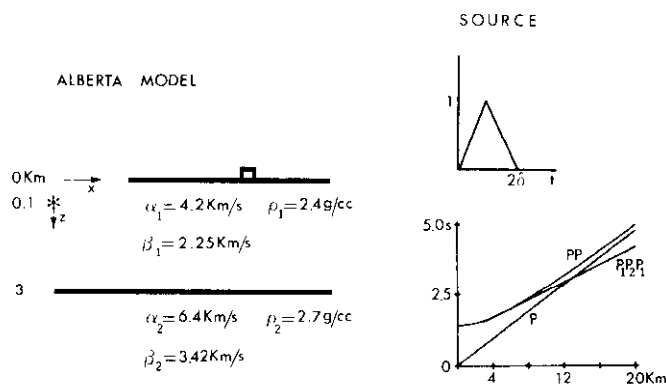


Fig. 1. Model of a layer over a half-space with the source at a shallow depth. The model simulates an "Alberta" sedimentary section with 4200 m/s Mesozoic sands and shales overlying a Paleozoic and Precambrian section with velocity of 6400 m/s. The source is a point vertical force at a depth of 100 m. The source function and the first part of the travel-time curve are shown on the right.

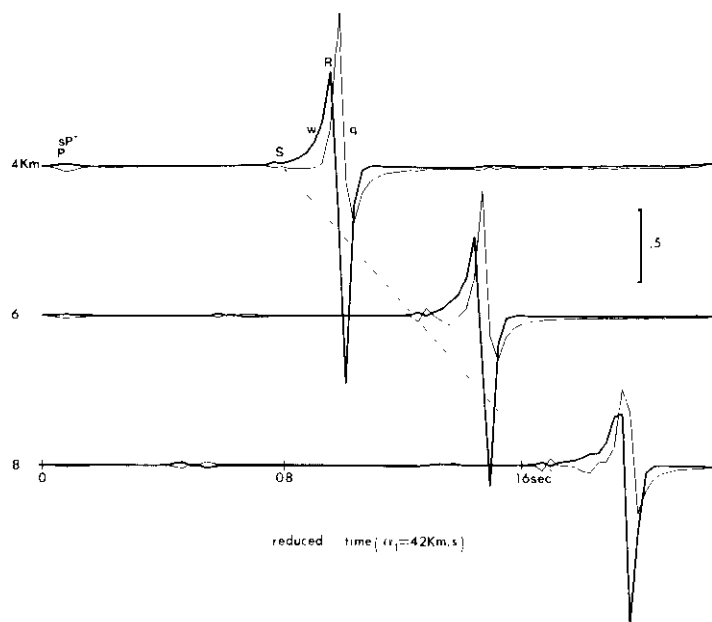


Fig. 2. Synthetic seismograms for the model shown in Figure 1. The radial and horizontal components are superimposed to show the phase relation for distances of 4 to 8 km from the source.

ings of Richards (1960) in the foothills belt of Stolberg over a distance range of 5.3 to 18.8 km.

The major event on the seismograms in Figure 3 is the PP reflection from the half-space. It is followed immediately by two generalized rays, sPP and pPP, which also have strong amplitudes. These two rays reflect off the surface close to the source. Their ray paths may be seen in Figure 4 under the third family, $F = 3$. Their visible effect depends on the depth of the source and the roughness of the reflecting surface that could be modelled as a parameter. The theoretical relative strength of the interfering phases may be seen in Figure 5.

The synthetic seismograms in Figure 3 also show strong arrivals for the SP and PS phases (see the sec-

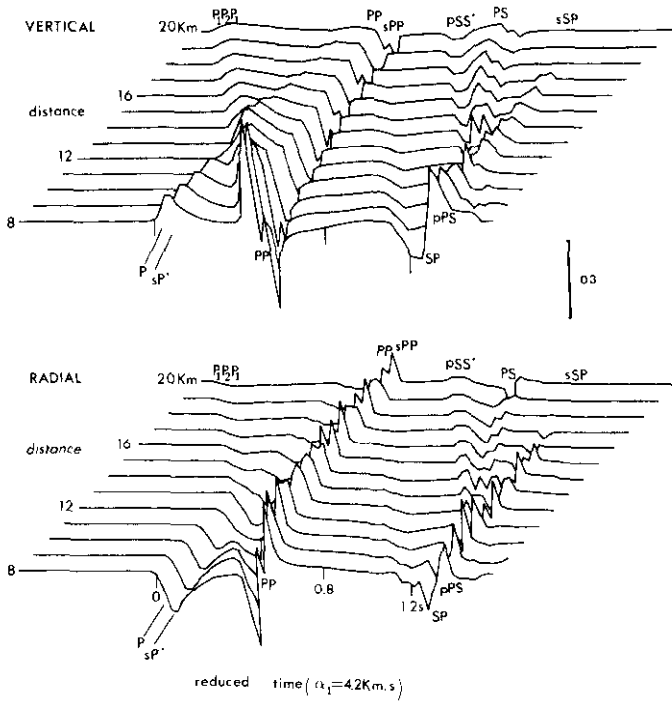


Fig. 3. Synthetic seismograms for a vertical point force and the model shown in Figure 1. The three-dimensional plot was made by using an algorithm called ASPEX and employs a reduction velocity of 4200 m/s. The head wave from the half-space is a first arrival beyond a distance of 13 km. The plot views the seismograms from an azimuth of 340°, an altitude of 18° from the horizontal at the centre of the graph to the observer, and a distance of 25 km from the graph to the observer.

ond family, $F = 2$, in Fig. 4). The SP ray occurs only at close distances, because a critical angle is reached when the compressional wave is travelling horizontally. At distances of 18 km the PS reflected ray may be interpreted. Note that the pSS* head wave in Figure 3 may be well enough defined to be of value in structural modelling. These head waves belong to the second and third families, with ray paths labelled $pS_1P_2S_1$ and $S_1P_2S_1$ in Figure 4.

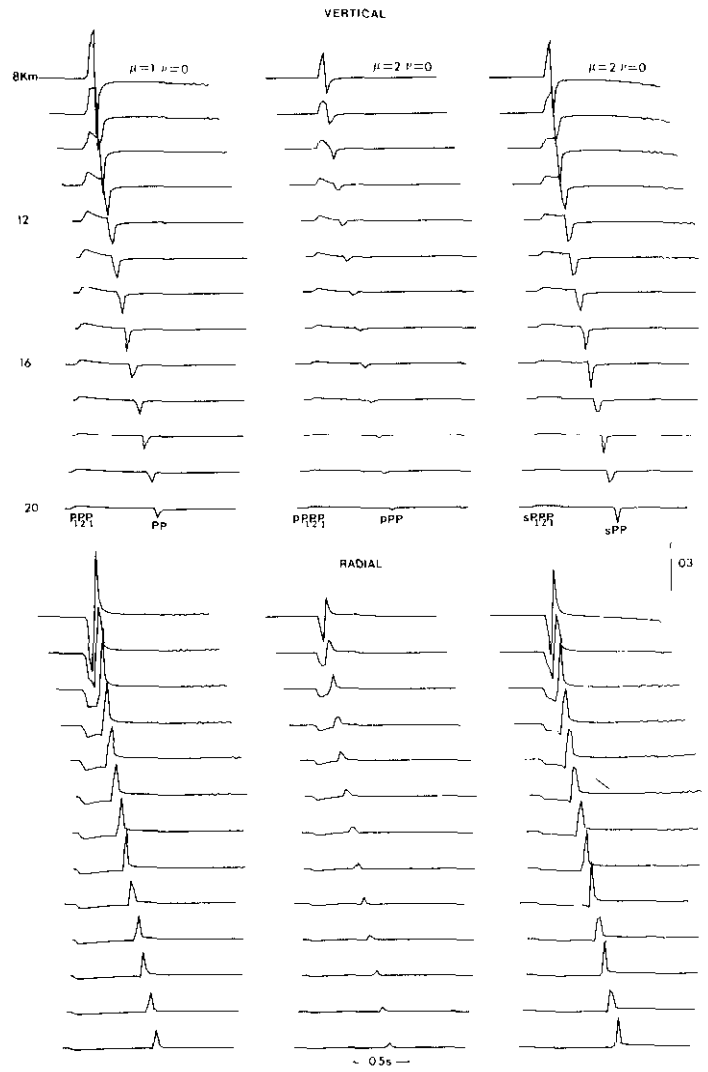


Fig. 5. The main reflected and head waves for the model in Figure 1. A superposition of these generalized rays and many other weaker ones make up the exact and complete seismograms up to a particular time in Figure 3.

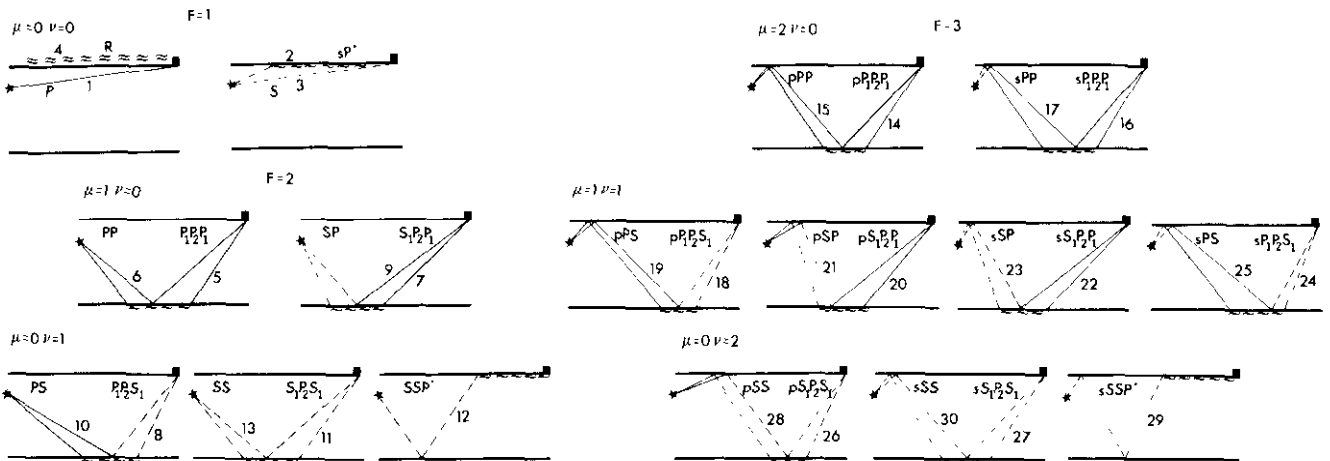


Fig. 4. Thirty ray paths for the first three families of rays. The parameter $F = (\mu + \nu + 1)$ is equal to the number of interactions the rays make with any available interface. The rays are also labelled by their traditional codes as P or S waves. Waves travelling upward initially from the source are indicated by lower-case p or s.

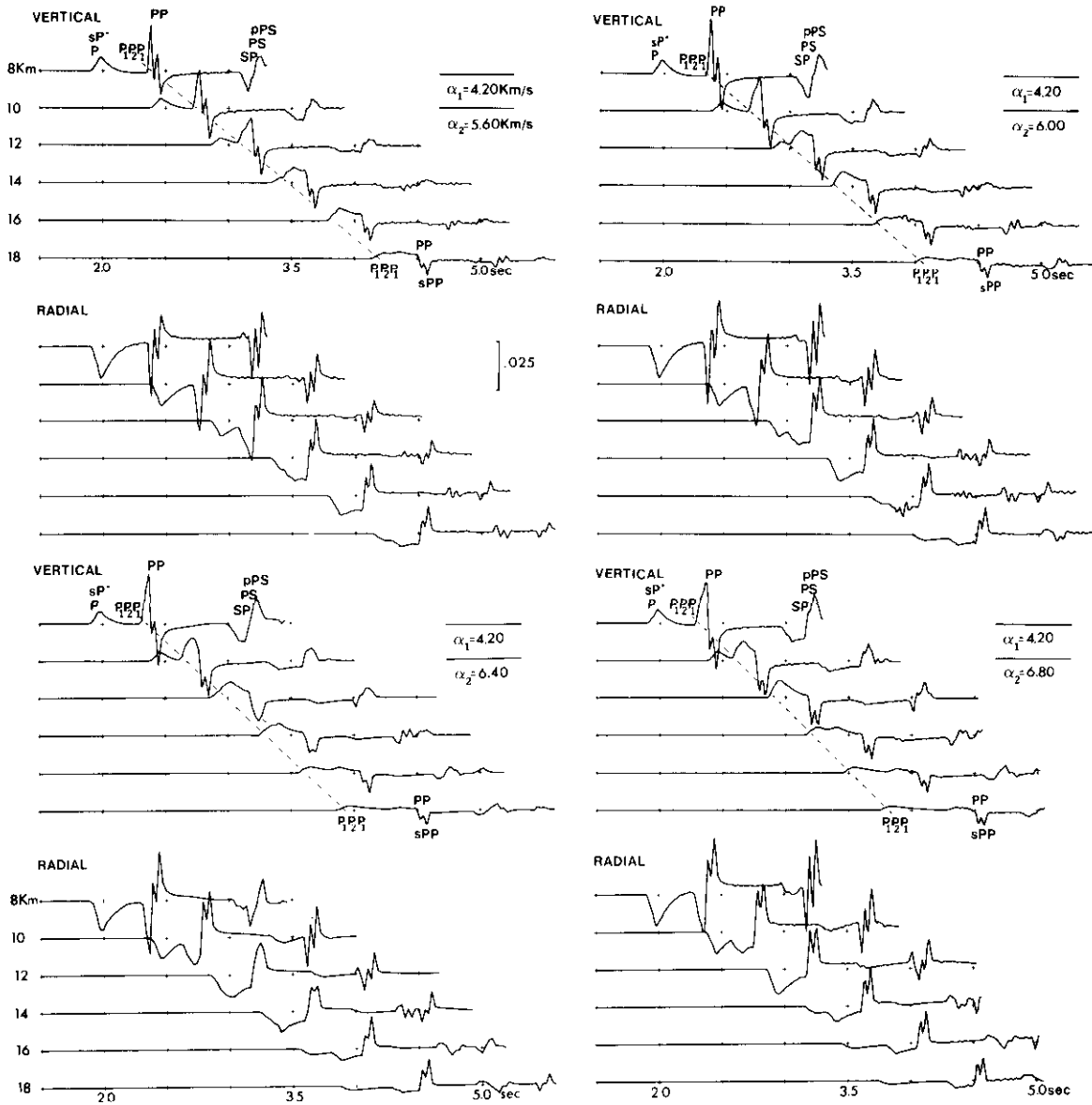


Fig. 6. Synthetic seismograms for a vertical point force and variations on the model shown in Figure 1. The only parameters that are changed are the P and S velocities in the second layer. The P velocities vary from 5600 to 6400 m/s and the S/P velocity ratio is 0.3.

The effect of changes in the velocity of the Paleozoic half space is shown in Figure 6. The interference of the direct P wave, the $P_1P_2P_1$ head wave, and the PP reflection makes it imperative that an exploration program be carefully designed, based on the thickness and velocities encountered. Note that the radial component has well-defined impulsive phases and it would be advantageous to record on horizontal-motion seismometers when carrying out seismic surveys for wide-angle reflections. The results from Figures 5 and 6 show that the source should be kept at as uniform and shallow a depth as possible, to avoid the interference created by sPP and pPP rays with the primary reflection, PP. A pattern of multiple sources would also help reduce the interference of converted and direct shear waves.

Attenuation and dispersion may be included in these synthetic seismograms. They are carried out individu-

ally on each generalized ray when in the frequency domain, through the use of a Fourier transform. The steps in the synthesis are shown in Figure 7. Each generalized ray is transformed by means of a fast Fourier transform (FFT). The absorption and dispersion along the rays is then introduced by using Futterman's well-known models. The effect of the viscoelastic interface is also taken into account by computing reflection coefficients with the use of complex elastic moduli. An inverse Fourier transform is then taken to return to the time domain, and all the generalized rays are summed to obtain the final synthetic seismogram up to any desired time.

The effect of attenuation is best illustrated on a near-surface or weathered-layer model where the attenuation is large. The characteristics of a weathered layer are idealized in Figure 8. A thin layer of low-

ATTENUATION — DISPERSION

- 1. ALONG THE PATH
- 2. INTERFACE

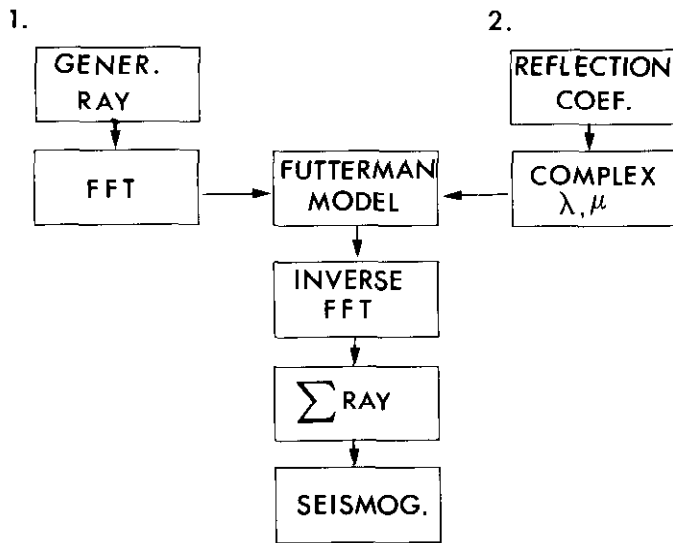


Fig. 7. Flowchart illustrating the algorithm for computing synthetic seismograms with attenuation.

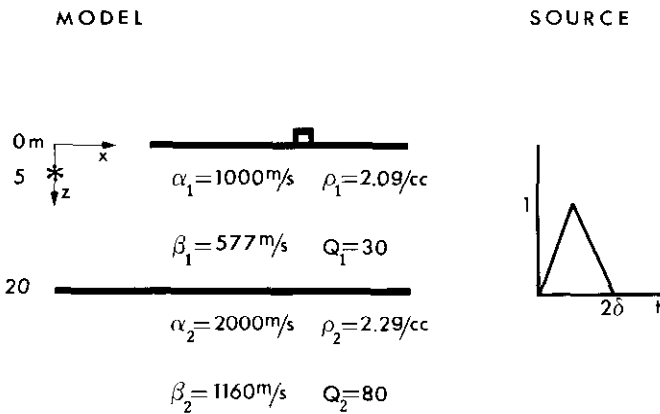


Fig. 8. Model of a layer over a half-space with the source at a shallow depth. The model is used for wave simulation in a weathered layer. The source is a stress impulse with a triangular shape in time. The attenuation is indicated by the quality factor Q.

velocity material overlies a thick high-velocity layer. Both layer and half-space have relatively low Q. Synthetic seismograms for a point vertical force are shown for surface vertical recording seismometers. The Rayleigh wave is very strong and completely dominates the seismograms with attenuation, which are labelled "anelastic" in Figure 9. Attenuation degrades the high-frequency impulsive reflected and head waves, and leaves the low-frequency surface waves altered only slightly. For a buried source the emergent Rayleigh wave (R) precedes and overlaps the direct shear wave arrival (S).

A new "surface head wave" labelled sP^* is seen in Figure 9. Its ray path is shown in the first family, $F = 1$, in Figure 4. The ray is generated by either a horizontal or a vertical stress pulse and does not occur when a purely compressive impulse is generated. The sP^* head wave travels as an S wave to the surface and is diffracted along the surface as a P or compressional wave. It was first predicted theoretically by Petrashin (1959) who called it a shear head wave. Numerical seismograms of this diffracted phase were first computed by Agramovici and Gal-Ezer (1978). It decays at $1/r^2$ and is 180° out of phase with the direct P and S wave. It is more prominent on the horizontal radial component than on the vertical receiver. Its effects may also be seen in Figure 3 immediately after the direct P arrival.

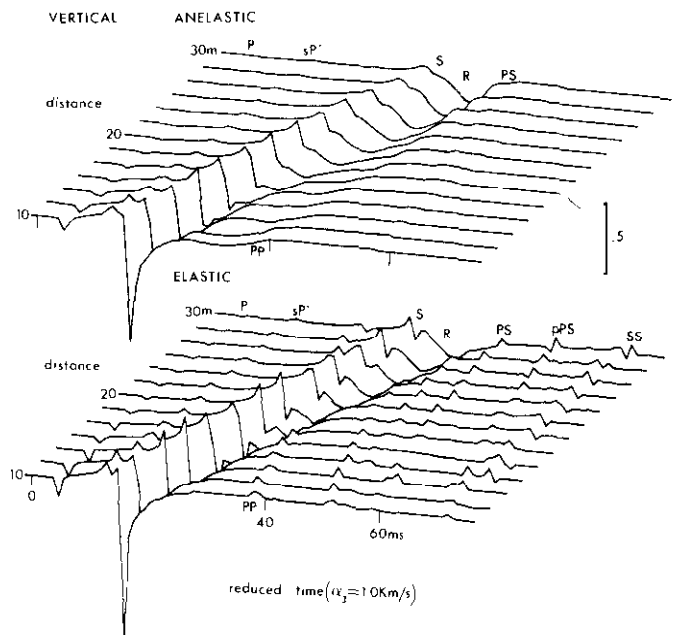


Fig. 9. The vertical component for the model in Figure 6 with a vertical point force. The upper group of seismograms incorporates attenuation whereas the lower set is for an elastic layered model with no attenuation ($Q = \infty$). The figure is viewed for an azimuth of 340° , an altitude of 18° from the horizontal at the centre of the graph to the observer, and a distance of 25 m from the graph to the observer in a three-dimensional plot using ASPX.

CONCLUSIONS

It is useful to obtain exact synthetic seismograms for an impulsive point vertical force by using generalized ray theory and an algorithm that performs an inverse Laplace transform. Decomposition into generalized rays allows one to analyze component phases and introduce the effects of attenuation. The simple model of a layer over a half-space is the first stage in analyzing more complex structures. These structures will require simplifying assumptions to make the computational time reasonable on present computers. The exact seismograms obtained in the analysis will serve as a check on results from more-complex layered structures.

REFERENCES

- Abramovici, F., 1970, Numerical seismograms for a layered elastic solid: *Bulletin of the Seismological Society of America*, v. 60, p. 1861-1876.
- _____, 1978, A generalization of the Cagniard method: *Journal of Computational Physics*, v. 29, p. 328-343.
- _____, and Gal-Ezer, J., 1978, Numerical seismograms for a vertical point force in a single layer over a half space: *Bulletin of the Seismological Society of America*, v. 68, p. 81-101.
- _____, Kanasewich, E. R. and Kelamis, P. G., 1982, Seismic waves from a horizontal stress discontinuity in a layered solid: *Bulletin of the Seismological Society of America*, v. 72, p. 1483-1498.
- Blundun, J. G., 1959, The Mississippian in the Alberta plains and the reflection seismograph: *Geophysics*, v. 24, p. 426-442.
- Cagniard, C. L., 1939, *Reflexion et Refraction des Ondes Seismiques Progressives*, Gauthier-Villars, Paris, France.
- Futterman, W. I., 1962, Dispersive body waves: *Journal of Geophysical Research*, v. 67, p. 5279-5291.
- Pekeris, C. L., Alterman, Z., Abramovici, F. and Jarosch, H., 1965, Propagation of a compressional pulse in a layered solid: *Reviews of Geophysics and Space Physics*, v. 3, p. 24-47.
- Petrashin G. C., 1959, *Elements of the Dynamic Theory of the Propagation of Seismic Waves: Part 1 in Collection III*, edited by G. Petrashin, Leningrad University, p. 11-106.
- Richards, T. C., 1960, Wide angle reflections and their application to finding limestone structure in the foothills of western Canada: *Geophysics*, v. 25, p. 385-407.
- _____, 1961, Motion of the ground on arrival of reflected longitudinal and transverse waves at wide angle reflection distances: *Geophysics*, v. 26, p. 277-297.